JOURNAL OF SPACECRAFT AND ROCKETS
Vol. 42, No. 5, September–October 2005

Dynamic Wrinkle Reduction Strategies for Cable-Suspended Membrane Structures

Hiraku Sakamoto* and K. C. Park†
University of Colorado, Boulder, Colorado 80309-0429
and
Yasuyuki Miyazaki‡
Nihon University, Chiba 274-8501, Japan

The present study addresses vibration mitigation of membrane structures the boundaries of which are surrounded by weblike perimeter cables. This proposed membrane design realizes significant structural mass reduction when compared to the conventional catenary design. A key dynamic characteristic of the proposed structure is that support perturbations propagated into the outer perimeter cables have a minor effect on the vibration frequencies of the membrane. This property has been exploited in the development of vibration mitigation strategies using active control. This is corroborated by carrying out nonlinear transient analysis, which accounts for the effect of wrinkles in the membrane. The results confirm that disturbances emanating from the support structures can be isolated by the outer perimeter cables while maintaining the interior membrane in a wrinkle-free taut condition. A simple active control law has been developed and applied to only the outer perimeter cables. Numerical simulations show that the combination of the web-cable girded membranes and the proposed vibration mitigation strategy can provide sufficient damping for both in-plane and out-of-plane vibrations.

Nomenclature

A	=	cross-sectional area of cable
$\boldsymbol{A}$	=	state matrix
a_0	=	stiffness-proportional damping matrix coefficient
$\boldsymbol{B}$	=	control influence matrix
D	=	length of a membrane side
$\boldsymbol{D}$	=	damping matrix
E	=	Young's modulus
$\boldsymbol{G}$	=	one-half of the critical damping matrix
$\boldsymbol{H}$	=	frequency-response function
H_{kl}	=	component of $\boldsymbol{H}$ in kth row and lth column
h	=	thickness
$\boldsymbol{I}$	=	identity matrix
J	=	scalar performance/cost index
J_u	=	control effort
j	=	imaginary number, $\sqrt{-1}$
$\boldsymbol{K}$	=	stiffness matrix
k	=	degree of freedom for output
$\boldsymbol{L}_a$	=	actuator influence matrix
l	=	degree of freedom for input
$\boldsymbol{M}$	=	mass matrix
$\boldsymbol{P}$	=	Riccati matrix for optimal control
p	=	height from membrane edge to support point
$\boldsymbol{Q}$	=	state weighting matrix
q	=	length of shortest tie cable
$\boldsymbol{q}$	=	nodal displacement vector
$\boldsymbol{R}$	=	control input weighting matrix
t	=	time
$\boldsymbol{u}$	=	control input vector
u	=	displacement of rhombic deformation
v_0	=	initial velocity
$\bar{X}$	=	normalized magnitude
x, y, z	=	Cartesian coordinate
$\boldsymbol{x}$	=	state vector
α	=	scalar weighting of strain energy
β	=	scalar weighting of kinetic energy
ϵ	=	strain
ζ	=	damping ratio
η	=	scalar proportional control gain
θ	=	central angle for inner catenary cable arc
ν	=	Poisson's ratio
ξ	=	scalar rate control gain
ρ	=	density
τ	=	dummy variable
ω	=	frequency

Subscripts

ic	=	inner catenary cable
m	=	membrane
opc	=	outer perimeter cable

Presented as Paper 2004-1581 at the AIAA/ASME/ASCE/AHS/ASC 45th Structures, Structural Dynamics, and Materials Conference, Palm Springs, CA, 19–22 April 2004; received 4 June 2004; revision received 12 February 2005; accepted for publication 4 March 2005.

*Graduate Research Assistant, Center for Aerospace Structures and Department of Aerospace Engineering Sciences, UCB 429; Hiraku.Sakamoto@Colorado.edu. Student Member AIAA.

†Professor, Center for Aerospace Structures and Department of Aerospace Engineering Sciences, UCB 429. Associate Fellow AIAA.

‡Associate Professor, Department of Aerospace Engineering, College of Science and Technology, 7-24-1 Narashinodai, Funabashi.

Introduction

MEMBRANE structures, such as solar sails and large reflectors, have been recognized as viable space structures. In most applications, wrinkles in the membrane can significantly degrade the structural performance. For example, membrane reflectors for precision antennas[1,2] require minimal wrinkles for higher surface accuracy. Likewise, wrinkles in solar sails may reduce the thrust and controllability.[3,4] However, because membrane wrinkles are a phenomenon involving highly nonlinear behavior, passive and active control employing linear models for wrinkling mitigation is not well understood. This is compounded by the fact that membranes are very flexible and very slightly damped and, thus, easily subjected to vibration.

One available and prevailing approach has been to maintain a wrinkle-free taut condition in membranes during their operation by using catenary cables along the membrane edges.[4–6] This approach

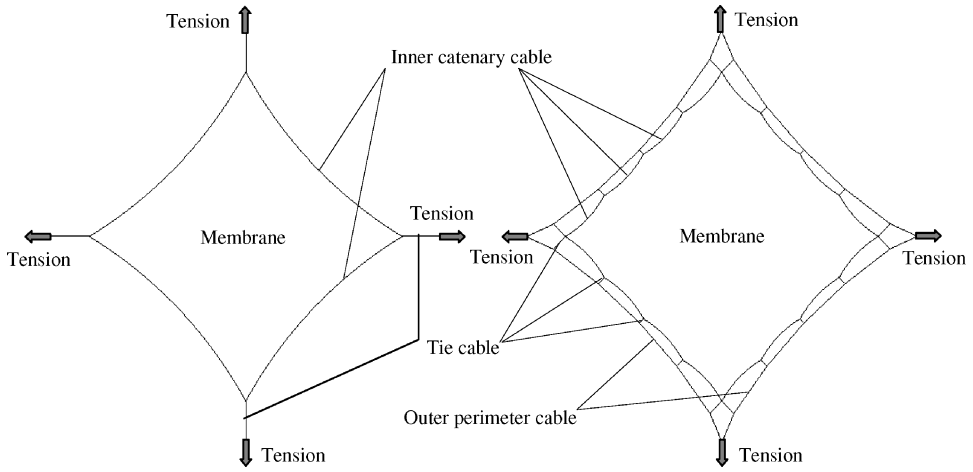

a) Conventional catenary design **b) Web-cable girded design**

Fig. 1 Conventional catenary design and proposed web-cable girded design.

has been found, however, to require high rigidity of the embedded catenary cables, as well as high stiffness of the support structure, which in turn results in a high-weight penalty in the overall system. In a previous study,[7] the authors proposed surrounding the membrane structure with weblike cables along the membrane perimeter. This design concept (Fig. 1b), when compared with a single catenary cable in conventional catenary design (Fig. 1a), has been found to possess three desired properties: 1) The proposed web-cable girded design requires far thinner boundary cables than the conventional catenary design, resulting in significantly less structural weight. 2) The outer perimeter cables can be exploited to absorb the brunt of disturbances emanating from the support points, thus alleviating wrinkling in the membrane. 3) The relative robustness against wrinkling enables a reduction in corner cable tensions so that the weight of the support structure booms can be reduced as well. Encouraged by these favorable properties, the present study explores the feasibility of employing linear theory-based active control, applying them primarily along the outer perimeter cables. Note that cables conceived in the present study are not necessarily of the classical type. Instead, they can be made of membrane strips and/or combinations of membrane strips and thin cables spread over membrane strips.

The significant aspect of the present paper is to establish a feasible strategy for suppressing vibration and mitigating wrinkles in membrane structures, based on the observations not only in linear vibration analysis, but also in nonlinear transient analysis. In both kinds of analyses, the effect of wrinkles in a membrane is taken into account by employing tension-field-theory-based membrane elements. The transient analysis of wrinkled membranes has been rarely studied to date, as summarized in the background section. Additionally, the proposed vibration suppression strategy associates only low-order linear theory-based controllers. Hence, the proposed strategy is innovative in enabling the vibration suppression of membrane structures with very simple linear controllers, without resorting to nonlinear controllers or linear controllers with high orders.

To this end, the authors have conducted the present study as follows. First, the impact of wrinkling in a membrane on its dynamic response under support point perturbations is investigated through linear vibration analysis using a finite element model that accounts for the effect of wrinkling. This investigation has shown that both the wrinkling regions and the frequencies of the proposed web-cable girded design changed very little, whereas those of the conventional design changed drastically. These observations suggest that, although membranes still exhibit significant nonlinear responses due to wrinkling, the outer perimeter cables mostly behave within linear ranges in the proposed design. This has been verified through a series of nonlinear dynamic analyses, which also accounts for wrinkling. Thus, it has been possible for the present authors to apply linear-theory-based vibration mitigation, primarily by application along the outer perimeter cables. This represents a significant simplification. A simple vibration suppression strategy, such as the Belvin–Park approach,[8] has been implemented to assess the effectiveness of active control. The numerical simulations demonstrate that vibration emanating from support perturbations in the proposed web-cable girded design can be effectively mitigated by applying linear active control along only the outer perimeter cables.

Background

Design Study of Membrane Structures

To apply a uniform prestrain in the membrane for space structures, introduction of single catenary cables along the membrane edge have been discussed,[4–6] and some engineering models have been constructed and tested on the ground.[9–13] However, these designs, termed conventional catenary in the present paper, require thick catenary cables as the bay width increases, because the required cable rigidity is proportional to the bay width.[7]

By contrast, the proposed web-cable girded design (Fig. 1b) realizes a uniform prestress state throughout a membrane with minimal cable mass. Design sketches similar to the proposed design are found by Miura and Natori.[14] Based on their design concept, a 3-m triangle membrane array was constructed for an in-orbit experiment and launched in March 1995.[15,16] The array was successfully deployed and retracted in orbit, and the unit was returned to the ground in January 1996. The experiment proved the viability of membrane space structures; however, more thorough studies are required for larger membranes and longer missions. In a similar approach, Talley et al.[3] and Leifer et al.[17] proposed the continuum shear compliant border around the membrane edges, and static analyses have been carried out.

The present study implements a dynamic analysis of the proposed web-cable girded design. Its wrinkling mitigation feature is enhanced by the introduction of inner catenary cables when compared with the design by Miura and Natori. Furthermore, the separation of the outer perimeter cables from the membrane boundaries facilitates vibration suppression strategies in only the outer perimeter cables.

Dynamic Analysis of Membrane Structures

Many experimental studies on membrane space structures have been done on the ground.[18–22] However, because simulating a microgravity and vacuum environment is difficult on the ground, numerical analysis of membrane dynamics will greatly complement the experimental studies. The recent development of a geometrically nonlinear finite element method has enabled the analysis of wrinkled membranes, and some researchers have utilized finite element techniques for the dynamic analysis of membrane structures as summarized as follows.

Currently, most finite element wrinkle modeling modifies the stress–strain relationship in the plane stress membrane element,

based on the assumption that the membrane does not support any compressive stress. This represents the so-called tension-field theory. Miller and Hedgepeth[23] originally formulated a wrinkled constitutive behavior for the finite element method. Jenkins and Leonard[24] first carried out dynamic transient analysis of a cantilever inflatable tube using a variable constitutive relation. Miyazaki and Nakamura[25] and Liu et al.[26] introduced penalty parameters into a wrinkled constitutive matrix to stabilize the numerical computation. Adler et al.[27] and Adler and MikuLas[28] implanted the Miller–Hedgepeth formula into commercial finite element codes, and Johnston[29] used Adler's method for a modal analysis of a subscale sunshield of the Next Generation Space Telescope (NGST) and compared it with ground testing to demonstrate good correlation in the global modes.

Kukathasan and Pellegrino[30] have conducted linear and nonlinear vibration analysis of a four-corner supported square membrane using three-dimensional thin-shell elements, another wrinkling modeling technique, and verified their analysis results with experiments. They showed that, as wrinkles get larger, the mode and mode shapes of the membrane become less predictable by unwrinkled models. The shell modeling provides detailed wrinkle information (amplitude, wavelength, and number of wrinkles), whereas the tension-field theory modeling only provides region and direction of wrinkles. However, the shell element model requires an extensive computational effort.

Therefore, because the present study focuses on the dynamic analysis, especially the transient response of the overall membrane structure, and does not require detailed wrinkle information, the tension-field-theory-based wrinkle model is chosen. Miyazaki and Nakamura's method,[25] which is adopted in the present study, employs an energy momentum method for dynamic analysis. The analysis model provided good agreement with the results of an inflatable tube deployment experiment in a microgravity environment.[31] All of the codes are handwritten on MATLAB®. Membranes are modeled in the present study by four-node quadrilateral elements whose constitutive relation is modified based on the tension-field theory assumption.

Linear Vibration Analysis of Web-Cable Girded Design

Linear Approximation

Although, in general, geometrical nonlinearity has to be taken into account in a membrane dynamic analysis, a linear approximated analysis will provide useful information for structural design under appropriate assumptions. In this section, the membrane structures are approximated as linear systems and conventional vibration analysis, modal and frequency-response analysis, is carried out. From the results, strategies for wrinkling mitigation and vibration suppression are discussed, which are applied in the transient analysis described in the following section.

When the two assumptions 1) small deformation and 2) wrinkles in the membrane do not move due to the deformation are made, the dynamics of a membrane structure in the finite element method can be approximated by a linear equation of motion:

$$\boldsymbol{M}\ddot{\boldsymbol{q}} + \boldsymbol{D}\dot{\boldsymbol{q}} + \boldsymbol{K}\boldsymbol{q} = 0 \tag{1}$$

where $\boldsymbol{K}$ is the tangent stiffness matrix. These matrices are obtained by a finite element model in a static equilibrium state. As discussed in the Background section the present study employs tension-field-theory-based membrane elements. Therefore, the tangent stiffness matrix $\boldsymbol{K}$ in Eq. (1) already contains the effect of wrinkles due to a nonuniform stress distribution in the membrane.

For the damping matrix in Eq. (1), the following conventional stiffness-proportional damping is used in the analysis for this section:

$$\boldsymbol{D} = a_0\boldsymbol{K} \tag{2}$$

where the coefficient a_0 is chosen by[32]

$$a_0 = 2\zeta/\omega_1 \tag{3}$$

Table 1 Material and design parameters in the analysis

Parameter	Value
Membrane (Kapton)	
E_m	2.5 GPa
h_m	25 μm
ν	0.3
ρ_m	1.42 g/cm^3
Cables (Kevlar)	
E_{ic}, E_{opc}	112.4 GPa
ρ_{ic}, ρ_{opc}	1.44 g/cm^3
Design	
θ	30 deg
p	$D/8$
q	$p/5$
ϵ_m, ϵ_{ic}	0.001%
ϵ_{opc}	0.1%

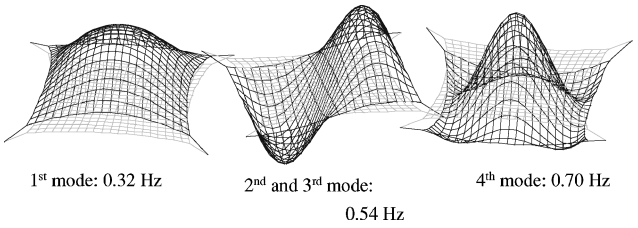

a) Conventional catenary design

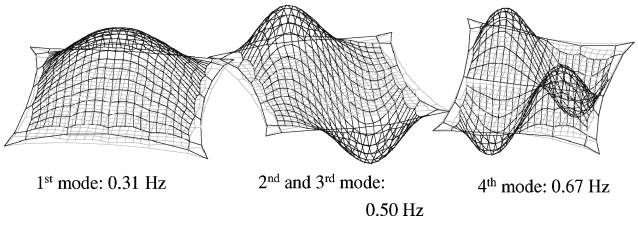

b) Web-cable girded design

Fig. 2 Mode frequencies and mode shapes of full models in ideal state.

where ω_1 is the first mode frequency of the system. The damping ratio ζ is chosen as $\zeta = 0.1\%$ throughout the analysis.

Modal Analysis

The mass and tangent stiffness matrices are constructed for both the conventional catenary design model and the web-cable girded design model in an ideal state, where the membrane is uniformly biaxially stressed. The design and material parameters used in these models are shown in Table 1. The membrane size is chosen as 10×10 m. For simplicity, only square membrane designs are discussed, and uniform cables are used for both outer perimeter cables and the tie cables, whose diameter is determined by the maximum tension in the outer perimeter cables, which occurs at the corners.

Eigenvalues and eigenvectors are computed for both models. The first four mode frequencies and mode shapes are shown in Fig. 2. As seen, the mode frequencies in both models are very close, and the first two mode shapes look similar. However, the following two investigations reveal the differences between the dynamic characteristics of the conventional design and the proposed design.

Wrinkling Effect on Modes

First, the support points are perturbed from their initial positions, with the same displacement in both designs. As in the previous study,[7] an in-plane rhombic deformation of the square support structure is assumed. As shown in Fig. 3, the displacement at the corners that perturbed outward, u, is chosen as $u = 1$ mm for the both designs. The conventional design experiences the onset of global wrinkles in its membrane. In Fig. 3, wrinkle directions in wrinkling regions, which are predicted by the tension-field-theory-based

Table 2 Mode frequencies of perturbed models

	Conventional design, Hz		Proposed design, Hz	
Mode	Ideal state	Perturbed	Ideal state	Perturbed
First	0.32	0.82	0.31	0.31
Second	0.54	1.08	0.50	0.50
Third	0.54	1.26	0.50	0.50
Fourth	0.70	1.48	0.68	0.67

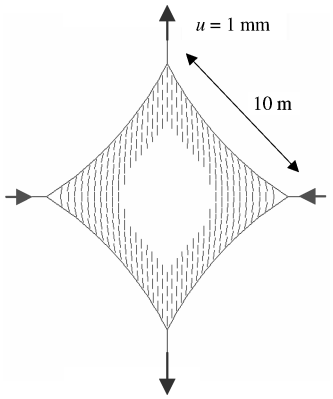

Fig. 3 Wrinkling region in conventional design subject to rhombic deformation.

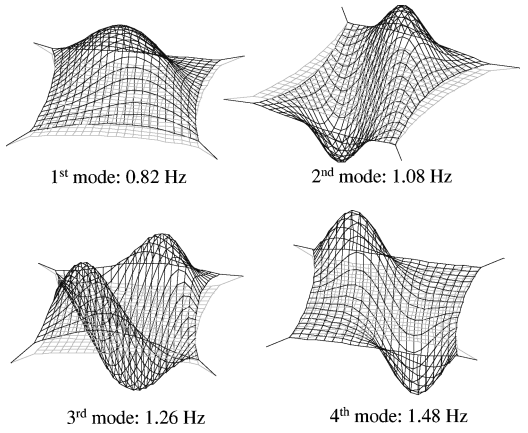

Fig. 4 Mode frequencies and mode shapes of conventional catenary design: support points perturbed.

elements, are shown by small lines inside the membrane. By contrast, in the proposed design, no wrinkles are observed in its membrane even under the same static disturbances. This result shows that the web cables (the outer perimeter cables and the tie cables) in the proposed design act for shear compliance. This effect provides a preferable dynamic characteristic to the proposed design, as discussed in the following paragraphs. Furthermore, this shear compliance effect in the web cables is also observed in the transient dynamic analysis in the following section.

With the perturbation at the support points, the mode frequencies and mode shapes of the conventional catenary design are drastically changed, as shown in Fig. 4. By contrast, the proposed design's mode frequencies and mode shapes are barely affected. The first four modes of both designs, with and without perturbations, are shown in Table 2. Note that the robustness feature against wrinkling of the proposed design keeps its dynamic response fairly predictable even under disturbances.

Partitioned Structural Analysis

Second, when only the cable networks or the membrane are partitioned in the web-cable girded design, the modal analysis of those substructural components provides interesting information. Figure 5 shows the mode frequencies and mode shapes of only the membrane elements and only the cable elements, extracted from the proposed design. As seen in Fig. 5, the mode frequencies and mode shapes of the membrane-only model (Fig. 5a) are very similar to those of the

Table 3 Modes of only outer perimeter cables in proposed web-cable girded design

	Modes, Hz		
A_{opc}, m^2	First	Second	Third
2×10^{-7}	18.9	27.0	40.0
2×10^{-8}	60.3	86.4	127.7

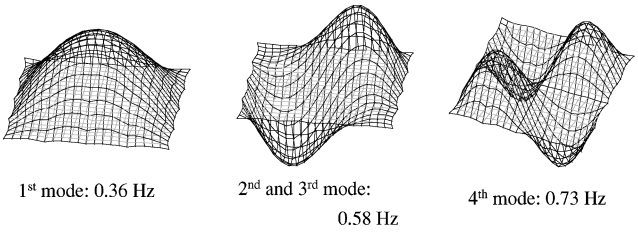

a) Membrane-only vibration

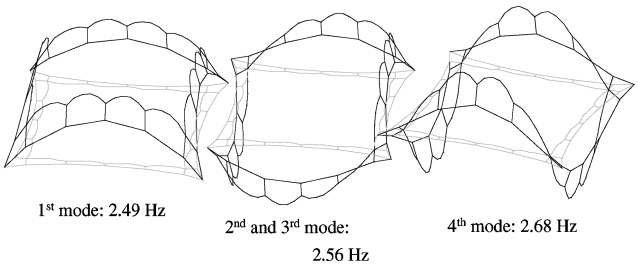

b) Cable-only vibration

Fig. 5 Mode frequencies and mode shapes of only membrane and only cables in proposed design.

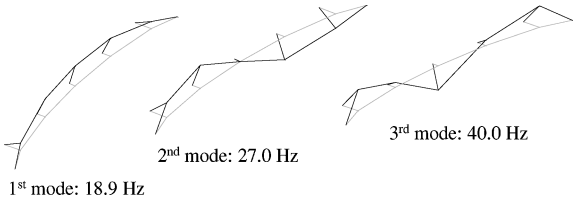

Fig. 6 Mode frequencies and mode shapes of only outer perimeter cables in proposed design.

full model (Fig. 2b). Thus, the global vibrational characteristics of the proposed design are dominated by the membrane component; however, locally the web cables have higher mode frequencies than the membrane, as shown in Fig. 5b. In space structures, the major vibration source is due to maneuvering of the spacecraft. Hence, most of the disturbances in the membrane are propagated from the vibrating support structures, which usually have higher inertia than the membrane. Therefore, the boundary layers around the membrane, with higher mode frequencies, will alleviate the propagation of undesired vibration from the support structures to the membrane interior.

Furthermore, when only the outer perimeter and tie cables are extracted from the proposed design, that is, no inner catenary cables, the components have still larger frequencies. Figure 6 and Table 3 shows the first three modes of one side, with only the outer perimeter and tie cables partitioned from the proposed design. Two important observations for vibration suppression of the proposed design can be derived from this outer perimeter cable analysis. First, as long as the cables do not slacken, the cable network is well approximated as a linear system. This observation enables the authors to apply linear-theory-based controllers in only the outer perimeter cables for vibration suppression of the overall structure.

Second, when it is recalled that the design strain in the outer perimeter cables can be set independently from the membrane design strain, the mode frequencies of the outer perimeter cable components can be actually tuned by designers. The standard design

strain in the outer perimeter cables in the present study is chosen as 0.1%, as shown in Table 1. This design strain corresponds to Kevlar® cables, whose cross-sectional area is 2×10^{-7} m^2, as in the top row of Table 3. When a larger strain is allowed in the outer perimeter cables, the cable cross-sectional area can be reduced. This increases the cable mode frequencies because the cable frequencies are inversely proportional to the square root of the cable cross-sectional area. For example, if the design strain is set at 1%, the required cable cross-sectional area is 2×10^{-8} m^2, and these cables give rise to an approximately $\sqrt{10}$ times larger mode frequencies than the standard model, as shown in the bottom row of Table 3. A 1% strain in Kevlar cables corresponds to a safety factor of 2.7, which is still an allowable value for spacecraft design.

However, high natural frequencies in the boundary layers are not always desirable from the control point of view. If the frequency difference between the membrane and the outer perimeter cables is too large, the vibration energy from the support structures will quickly flow into the low-frequency system, which is the membrane, thereby degrading the ability of control strategies implemented only in the boundary cable networks. Therefore, the outer perimeter cables have to be carefully tuned, depending on the control system introduced into the system.

Frequency-Response Function

The frequency-response function (FRF) of both designs for a 10×10 m square membrane is computed. FRF is given by

$$\boldsymbol{H}(\omega) = [(j\omega)^2\boldsymbol{M} + (j\omega)\boldsymbol{D} + \boldsymbol{K}]^{-1} \tag{4}$$

In-plane and out-of-plane FRF at node B for the unit input applied at node E, where both node locations are shown in Fig. 7, is obtained for both the conventional catenary design and the web-cable girded design. The magnitude of FRF is normalized with respect to the static deformation amplitude at node E due to the unit force, which is given by $H_{ll}(0)$, as

$$\bar{X}(\omega) = |H_{kl}(\omega)|/|H_{ll}(0)| \tag{5}$$

where $\bar{X}(\omega)$ is the normalized magnitude for the frequency ω and k and l are the degrees of freedom at nodes B and E, respectively.

In-Plane FRF

Figure 8 shows the frequency response in x direction at node B both in the conventional and the proposed design. The solid line indicates the undamped response, and the dashed line indicates the damped response. The responses of both designs appear very similar. Except for the first few peaks in the very low-frequency range, the modes lie in a relatively higher frequency range (above 50 Hz) and they are sufficiently damped. However, it is well known that the stiffness-proportional damping used in the present analysis provides higher damping for high frequencies; thus, further investigation is required to show whether this damping model is physically valid.

However, it is still clear that, for in-plane vibration, the first few lowest modes are critical and the effect of the higher modes is not significant and may be ignorable. From this observation, one can expect that the controller designed by using a reduced-order model may be sufficient for in-plane active vibration suppression.

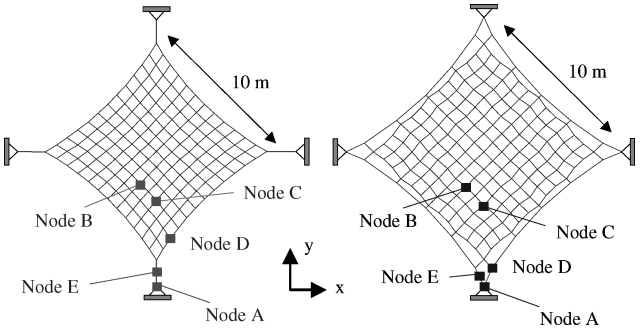

a) Conventional catenary design **b) Web-cable girded design**

Fig. 7 Finite element models for dynamic analysis.

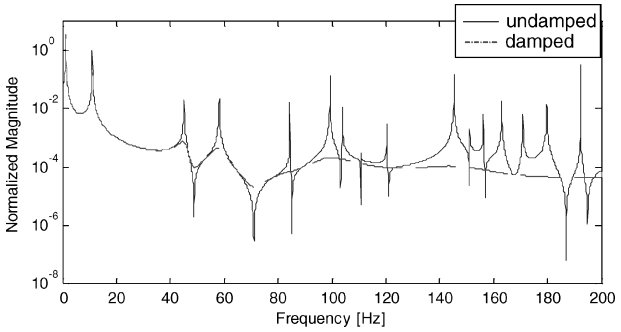

a) Conventional catenary design

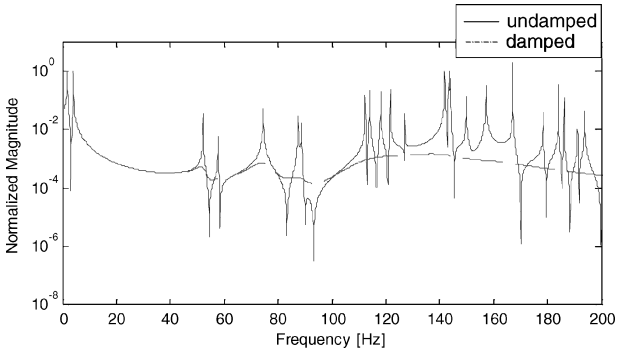

b) Web-cable girded design

Fig. 8 In-plane frequency response at node B in x direction for input at node E.

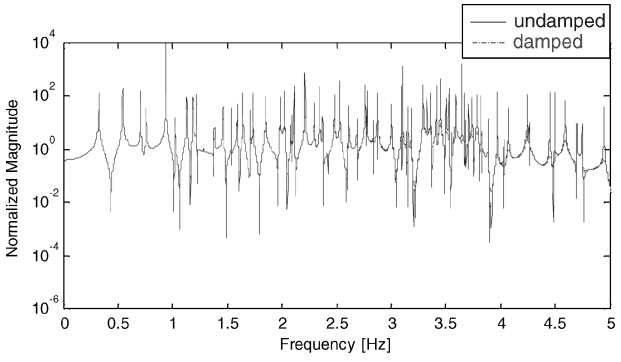

a) Conventional catenary design

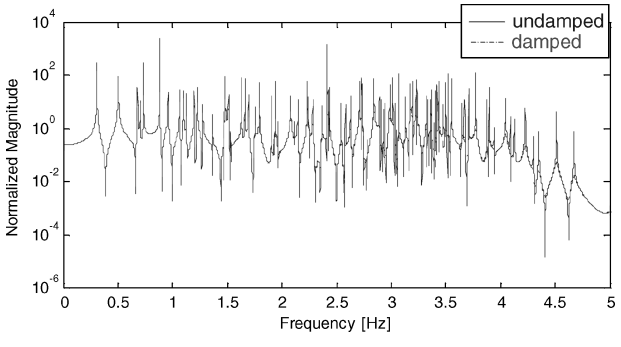

b) Web-cable girded design

Fig. 9 Out-of-plane frequency response at node B in z direction for input at node E.

Out-of-Plane FRF

Figure 9 shows the frequency response in the out-of-plane direction (z direction) at node B both for the conventional and the proposed design. Both responses look similar, and two things can be observed: First, many peaks are found in the very low-frequency

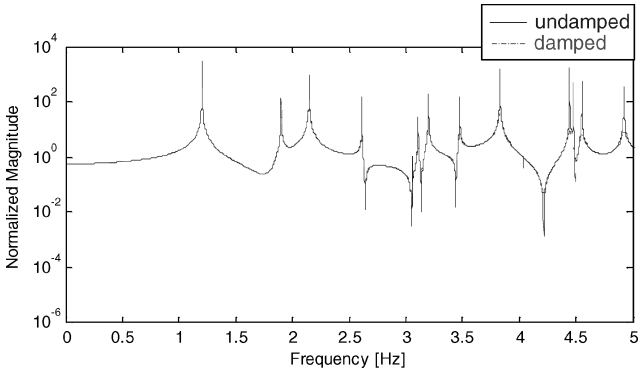

a) Conventional catenary design

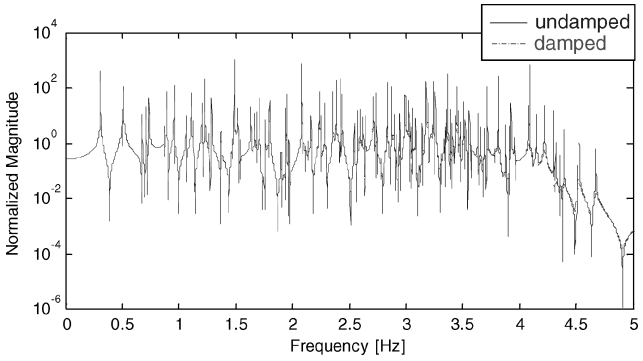

b) Web-cable girded design

Fig. 10 Out-of-plane frequency response for perturbed model at node B in z direction for input at node E: conventional design has wrinkles as shown in Fig. 3.

range (less than 5 Hz). Second, the effect of passive damping is very small. These results indicate that the out-of-plane vibration suppression is extremely difficult in both designs. However, because the membrane in the conventional design is prone to wrinkling, the control of the conventional design is far more difficult than control of the proposed design.

Figure 10 shows the frequency response of the models whose support corners are perturbed, as shown in Fig. 3. As discussed, the conventional design suffers a large wrinkling region. As a result, the response shown in Fig. 10a is substantially different from the ideal model (Fig. 9a). Because the membrane tension is tightened in this case, the system mode frequencies increased. As one can easily imagine, the frequencies decrease when the membrane is loosen. By contrast with the conventional design, the response of the proposed design is only slightly changed even under the same perturbation (Fig. 10b).

Therefore, the proposed design has less uncertainty in its dynamic response than the conventional design. This shows that a full-order model-based linear controller may provide sufficient vibration suppression in the proposed design. However, the realization of a full-order controller is very costly, or sometimes impossible. Thus, when it is considered that the linear approximation of the outer perimeter cables is reasonable, the outer perimeter cable substructure-based controller, which significantly reduces the controller order, is developed in the following section.

Nonlinear Transient Analysis of Web-Cable Girded Design

Impulse Transient Response

As discussed in the preceding section, the major disturbance input to the membrane structure emerges from the support points. For example, in a square solar sail design with crossing support booms, the effect on the membrane from boom vibration will be much larger than the effect of solar pressure. To simulate the dynamic response due to such disturbance input from the support structures, impulse velocity is applied at node A, as shown in Fig. 7, in both the conventional catenary design and proposed design, each with a 10×10 m square membrane. Then transient analysis is carried out by the geometrically nonlinear finite element method described in the "Background" section. The amplitude of the initial velocity at node A is chosen as $v_0 = 10$ m/s.

Uncontrolled Out-of-Plane Response

Figure 11 shows the time history of the out-of-plane displacement at node C (in the membrane interior) and node D (at the boundary), as shown in Fig. 7, in the conventional and the proposed design. The impulse velocity is applied at node A at $t = 0$. As can be seen, the conventional design experiences large displacements both in the interior and at the boundary, whereas in the proposed design, although the outer perimeter cables vibrate somewhat, the membrane remains very flat. This clearly shows that in the proposed design the vibration propagated from the support structures is absorbed by the outer perimeter cables before it reaches the membrane.

Figure 12 shows the wrinkling area in the membrane in both designs for the same simulation. The membrane in the conventional design suffers a wrinkling area encompassing 80% of the entire

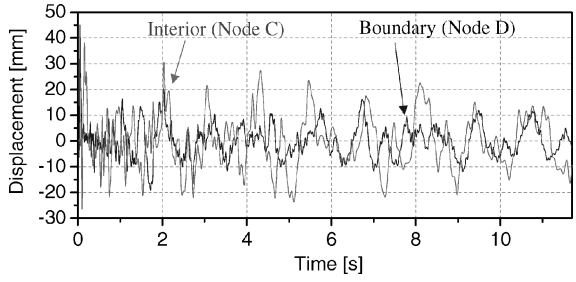

a) Conventional catenary design

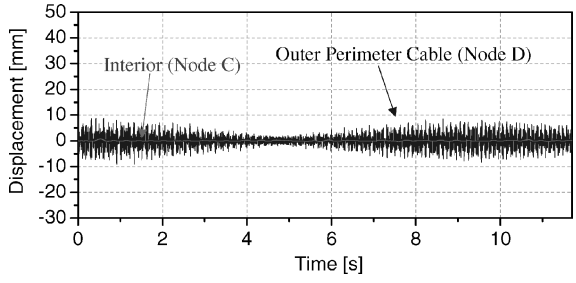

b) Web-cable girded design

Fig. 11 Out-of-plane transient response for impulse velocity applied at node A at $t = 0$.

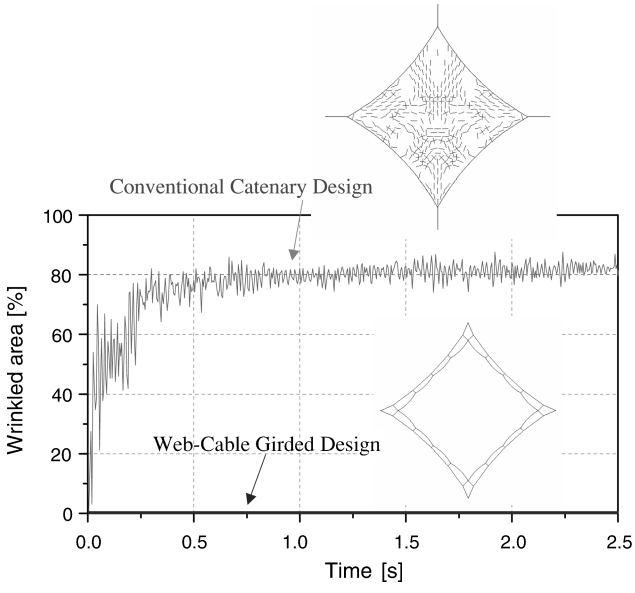

Fig. 12 Wrinkling area for impulse velocity applied at node A at $t = 0$.

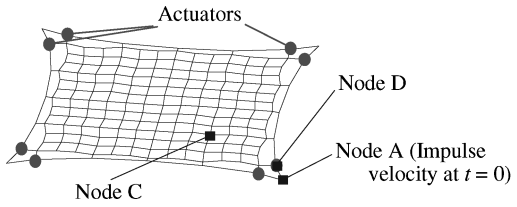

Fig. 13 Actuator locations in proposed design.

membrane; by contrast, the proposed design remains wrinkle free even for the same disturbance input. Thus, this transient analysis shows that the proposed design has the wrinkle mitigation ability not only for static perturbations but also for dynamic disturbances. This feature is enhanced by the introduction of active controllers along the outer perimeter cables as explored in the following subsection. In future studies, the impact of the design change in the web cables (topology, thickness, etc.) on this passive disturbance rejection effect will also be explored.

Active Vibration Suppression via Outer Perimeter Cables

Actuation of the interior membrane will be very difficult. Thus, the reasonable choice will be the actuation of the boundary cables. Natori et al.[33] proposed a membrane vibration suppression strategy that changes the tension level in the entire membrane. This nonlinear control is theoretically attractive; however, the practical realization will be very difficult. Solter et al.[34] have constructed a small actuator both for in-plane and out-of-plane vibration, which is introduced along the catenary cables. They demonstrated the single-input and single-output control for the membrane in a hexapod.

On the basis of the preceding discussion, the present authors propose the linear-theory-based multi-input and multi-output vibration mitigation, primarily applying it along the outer perimeter cables. The insights obtained from the analysis so far are as follows. For the in-plane vibration, vibration suppression is critical only for a few modes in the low-frequency range (Fig. 8b). Thus, a controller designed from a reduced-order model may be sufficient. For the out-of-plane vibration, the controller has to deal with many modes (Fig. 9b). Thus, a full-order controller is preferable. However, the outer perimeter cables in the proposed design, which are well approximated by a linear system (Fig. 6), absorb the vibration propagated from the support structures before it reaches the interior membrane (Fig. 11b). Therefore, as the simplest choice, a full-order linear controller is designed based only on the substructure component of the boundary cable networks, with the membrane left unmodeled.

To assess the effectiveness of the proposed active vibration suppression strategy, the present study utilizes the simple linear quadratic (LQ) optimal control as explained subsequently. Actuators, both for in-plane and out-of-plane vibration, are assumed to be located at eight points near the support corners, as shown in Fig. 13, for preliminary investigation. These controllers are installed into the finite element models, and the transient analysis is carried out.

Belvin–Park Controller

The LQ controller is designed according to Belvin and Park.[8] Similar to Eq. (1), the linearized equation of motion of the structure is given by

$$\boldsymbol{M}\ddot{\boldsymbol{q}} + \boldsymbol{D}\dot{\boldsymbol{q}} + \boldsymbol{K}\boldsymbol{q} = \boldsymbol{L}_a\boldsymbol{u} \tag{6}$$

where $\boldsymbol{u}$ is the actuator input vector and $\boldsymbol{L}_a$ is the Boolean matrix for the actuator location. Rewriting Eq. (6) into the state-space description yields

$$\dot{\boldsymbol{x}} = \boldsymbol{A}\boldsymbol{x} + \boldsymbol{B}\boldsymbol{u} \tag{7}$$

where

$$\boldsymbol{A} = \begin{bmatrix} \boldsymbol{0} & \boldsymbol{I} \\ -\boldsymbol{M}^{-1}\boldsymbol{K} & -\boldsymbol{M}^{-1}\boldsymbol{D} \end{bmatrix}, \qquad \boldsymbol{B} = \begin{bmatrix} \boldsymbol{0} \\ \boldsymbol{M}^{-1}\boldsymbol{L}_a \end{bmatrix}, \qquad \boldsymbol{x} = \begin{bmatrix} \boldsymbol{q} \\ \dot{\boldsymbol{q}} \end{bmatrix}$$

The following cost functional is set up:

$$J = \int_0^t \frac{1}{2}(\boldsymbol{x}^T\boldsymbol{Q}\boldsymbol{x} + \boldsymbol{u}^T\boldsymbol{R}\boldsymbol{u})\,\mathrm{d}\tau \tag{8}$$

where the weighting matrices $\boldsymbol{Q}$ and $\boldsymbol{R}$ are chosen as

$$\boldsymbol{Q} = \begin{bmatrix} \alpha\boldsymbol{K} & \boldsymbol{0} \\ \boldsymbol{0} & \beta\boldsymbol{M} \end{bmatrix}, \qquad \boldsymbol{R} = \boldsymbol{L}_a^T\boldsymbol{K}^{-1}\boldsymbol{L}_a \tag{9}$$

where α and β are the tuning parameters. With this choice, the minimization of the cost functional in Eq. (8) corresponds to the minimization of the internal energy in the system and the control effort simultaneously. Then the optimal feedback gain is given by

$$\boldsymbol{u} = -\boldsymbol{R}^{-1}\boldsymbol{B}^T\boldsymbol{P}\boldsymbol{x} \tag{10}$$

where $\boldsymbol{P}$ is the solution to the steady-state matrix Riccati equation,

$$\boldsymbol{0} = \boldsymbol{Q} + \boldsymbol{P}\boldsymbol{A} + \boldsymbol{A}^T\boldsymbol{P} - \boldsymbol{P}\boldsymbol{B}\boldsymbol{R}^{-1}\boldsymbol{B}^T\boldsymbol{P} \tag{11}$$

When $\boldsymbol{D} = 0$ is assumed, that is, neglecting structural damping, using the weighting matrices in Eq. (9), $\boldsymbol{P}$ can be explicitly expressed as

$$\boldsymbol{P} = \begin{bmatrix} 2\xi\boldsymbol{G} & \eta\boldsymbol{M} \\ \eta\boldsymbol{M} & \xi\boldsymbol{M}\boldsymbol{K}^{-1}\boldsymbol{G} \end{bmatrix} \tag{12}$$

where

$$\eta = \sqrt{1+\alpha} - 1, \qquad \xi = \sqrt{2\eta + \beta}$$

$$\boldsymbol{G} = \boldsymbol{M}^{\frac{1}{2}}\left[\boldsymbol{M}^{-\frac{1}{2}}\boldsymbol{K}\boldsymbol{M}^{-\frac{1}{2}}\right]^{\frac{1}{2}}\boldsymbol{M}^{\frac{1}{2}}$$

Transient Response with Active Control

In-Plane Vibration

The reduced-order model is constructed using a coarse mesh for the membrane, as shown in Fig. 14a. The in-plane controller is designed based on this reduced-order model, by use of the Belvin–Park approach. The displacement and velocity sensors are assumed to be located on all nodes along the outer perimeter cables and also at the center node of the membrane. The tuning parameters in Eq. (9) are chosen as $\alpha = \beta = 6 \times 10^{-4}$. Because the LQ controller requires full state feedback, the rest of the state is estimated by using a Kalman filter.

This controller is installed into the proposed design model, shown in Fig. 13, and the impulse velocity, $v_0 = 10$ m/s, is applied in the x direction at node A and at $t = 0$. Figure 15 shows the displacement time history in the x direction at node C (membrane interior) and node D (outer perimeter cable). As can be seen, the in-plane vibration is sufficiently damped by the LQ regulator introduced only near the support corners.

Figure 16 shows the time history of the force generated by the actuator in the x direction at node D. As can be seen, the control input is certainly bounded and decreases with time. A residual control input is observed because the reduced-order linear controller is used

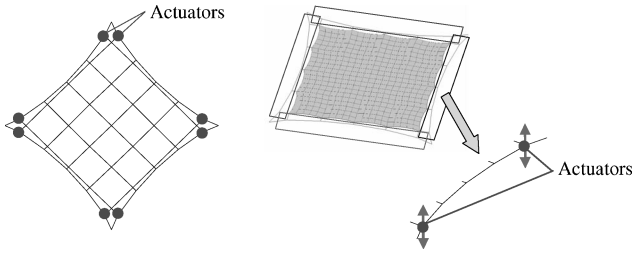

a) Reduced-order model for in-plane controller **b) Substructure for out-of-plane controller**

Fig. 14 Models used for controller design.

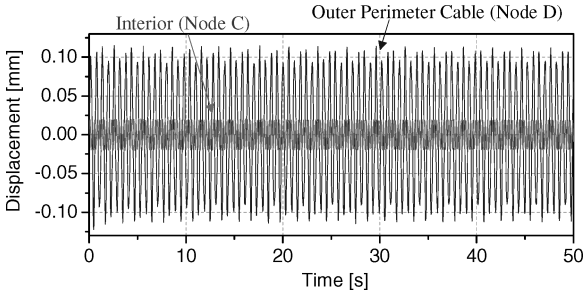

a) Without control

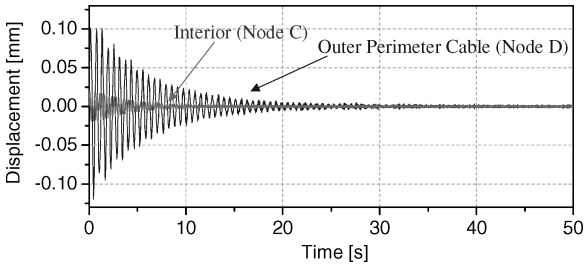

b) With control

Fig. 15 In-plane (*x*-direction) transient response of proposed design with active control along outer perimeter cables.

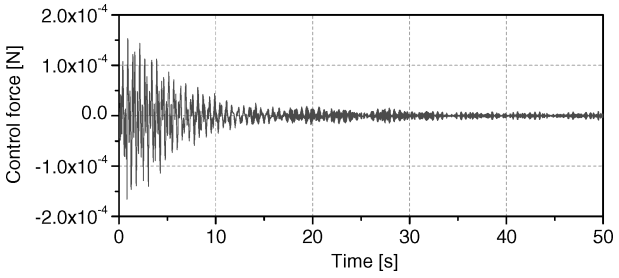

Fig. 16 In-plane actuator force at node D in *x* direction.

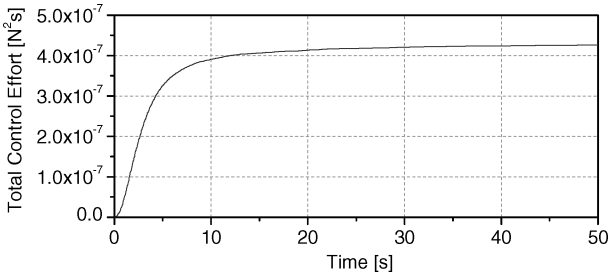

Fig. 17 Total control effort of in-plane controller.

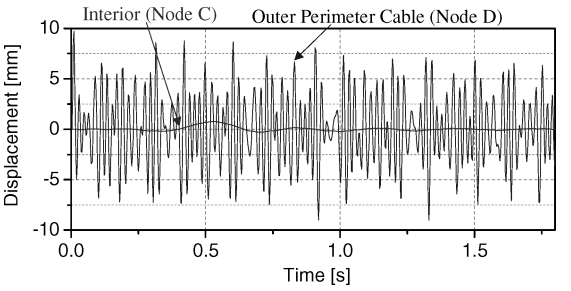

a) Without control

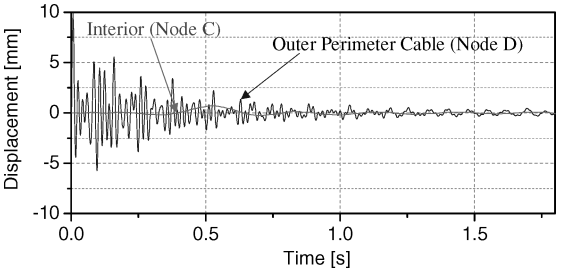

b) With control

Fig. 18 Out-of-plane transient response of proposed design with active control along outer perimeter cables.

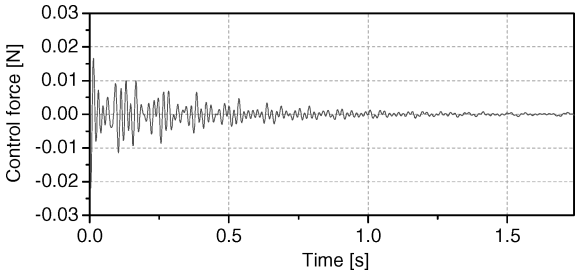

Fig. 19 Out-of-plane actuator force at node D.

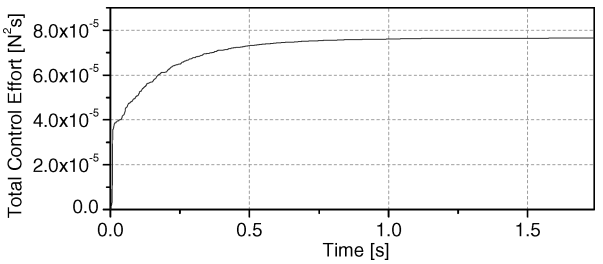

Fig. 20 Total control effort of out-of-plane controller.

for a nonlinear, higher-order system. Figure 17 shows the sum of the control effort of the 16 actuators (at 8 nodes for both the x and y directions). The control effort J_u is defined by

$$J_u = \int_0^t \boldsymbol{u}^T \boldsymbol{u}\, \mathrm{d}\tau \tag{13}$$

As shown in Fig. 17, after $t = 10$ s, the control input from all of the actuators is very small.

Out-of-Plane Vibration

Only the quarter-part of the boundary cable network is partitioned from the global system, as shown in Fig. 14b, and the full-order out-of-plane controller for the substructure is designed by use of the Belvin–Park method. The tuning parameters in Eq. (9) are chosen as $\alpha = \beta = 1 \times 10^{-2}$. Because the partitioned substructure is small, the obtained controller has a very low order. The out-of-plane displacement and velocity sensors are assumed to be located on the all nodes along the outer perimeter cables, thus, realizing full state feedback.

Four substructure-based controllers are installed into the outer perimeter cables along the four sides of the membrane. Figure 18 shows the out-of-plane control results. The vibration of the outer perimeter cable is well damped by the introduction of the eight actuators near the support corners. However, small residual vibration is observed. This is due to the effect of the unmodeled membrane dynamics, as well as the nonlinearity of the system.

The actuator force at node D is shown in Fig. 19. As seen in Fig. 19, the input is bounded and drops rapidly. Figure 20 shows the total control effort J_u, defined in Eq. (13), of the eight out-of-plane controllers. Because the structure has much less stiffness in the out-of-plane direction than in the in-plane direction, the out-of-plane controller must produce a control effort more than 100 times larger than the in-plane controller, as shown in Fig. 17.

Discussion

The present study paves the way for the vibration suppression of membrane structures using small-order linear controllers, without resorting to the use of nonlinear controllers or high-order linear controllers. However, to enhance the robustness of the controller, the membrane dynamics, which are left unmodeled in the present out-of-plane vibration suppression strategy, should be included in the controller. In addition, simultaneous optimization of the controller design and the structural design, especially the outer perimeter cable design around the membrane boundaries, should be addressed further. These topics are currently under investigation by the authors.

Conclusions

From the preceding discussion, we can conclude that the proposed web-cable girded membrane design enables the introduction of effective vibration suppression, as well as wrinkle reduction, strategies, using the linear-theory-based, low-order controllers installed along only the outer perimeter cables. Linear vibration analysis using finite element models, which account for the wrinkling effect, shows that the mode frequencies and mode shapes of membrane structures are drastically affected by the support point perturbations in the conventional catenary design; by contrast, those of the proposed design are barely changed. These observations enable the authors to apply linear-theory-based vibration control primarily to the outer perimeter cables in the proposed design. The controller order can be substantially reduced by the model reduction via a coarse finite element meshing and a substructure-based modeling. The series of nonlinear transient analyses, also considering wrinkling in the membranes, demonstrates that vibration emanating from support perturbations in the proposed web-cable girded design is sufficiently damped by the proposed vibration suppression strategies.

Acknowledgments

This research is partially supported by Research Grant NAG-1-02009 from NASA Langley Research Center. The authors thank M. C. Natori, Institute of Space and Astronautical Science, Japan; Sergio Pellegrino, University of Cambridge, Cambridge, England, U.K.; and Jason Hinkle, University of Colorado, for their helpful comments. We thank W. Keith Belvin for his encouragement and constructive technical discussions.

References

[1]Lin, J. K., Sapna, G. H., III, Scarborough, S. E., and Lopez, B. C., "Advanced Precipitation Radar Antenna Singly Curved Parabolic Antenna Reflector Development," AIAA Paper 2003-1651, April 2003.

[2]White, C., Salama, M., Hatheway, A., Dragovan, M., Schroeder, J., Barber, D., and Dooley, J., "Shaping of Parabolic Cylindrical Membrane Reflectors for the DART Precision Test Bed," AIAA Paper 2003-1652, April 2003.

[3]Talley, C., Clayton, W., Gierow, P., McGee, J., and Moore, J., "Advanced Membrane Materials for Improved Solar Sail Capabilities," AIAA Paper 2002-1561, April 2002.

[4]Mikulas, M. M., and Adler, A. L., "Rapid Structural Assessment Approach for Square Solar Sails Including Edge Support Cords," AIAA Paper 2003-1447, April 2003.

[5]Greschik, G., and Mikulas, M. M., "Design Study of a Square Solar Sail Architecture," *Journal of Spacecraft and Rockets*, Vol. 39, No. 5, 2002, pp. 653–661.

[6]Greschik, G., White, C. V., and Salama, M. A., "On the Precisely Uniform and Uniaxial Tensioning of a Film Sheet via Integrated Catenary," AIAA Paper 2003-1096, April 2003.

[7]Sakamoto, H., Miyazaki, Y., and Park, K. C., "Evaluation of Cable Suspended Membrane Structures for Wrinkle-Free Design," AIAA Paper 2003-1905, April 2003.

[8]Belvin, W. K., and Park, K. C., "Structural Tailoring and Feedback Control Synthesis: An Interdisciplinary Approach," *Journal of Guidance, Control and Dynamics*, Vol. 13, No. 3, 1990, pp. 424–429.

[9]Fang, H., Lou, M., Hsia, L., and Leung, P., "Catenary Systems for Membrane Structures," AIAA Paper 2001-1342, April 2001.

[10]Lopez, B. C., Lou, M. C., Huang, J., and Edelstein, W., "Development of an Inflatable SAR Engineering Model," AIAA Paper 2001-1618, April 2001.

[11]Fang, H., Lou, M., Huang, J., Hsia, L., and Kerdanyan, G., "Inflatable Structure for a Three-Meter Reflectarray Antema," *Journal of Spacecraft and Rockets*, Vol. 41, No. 4, 2004, pp. 543–550.

[12]Adetona, O., Keel, L. H., Horta, L. G., Cadgan, D. P., Sapna, G. H., and Scarborough, S. E., "Description of New Inflatable/Rigidizable Hexampd Structure Tested for Shape and Vibration Control," AIAA Paper 2002-1451, April 2002.

[13]Lichodziejewski, D., Cravey, and Hopkins, G., "Inflatably Deployed Membrane Waveguide Array Antenna for Space," AIAA Paper 2003-1649, April 2002.

[14]Miura, K., and Natori, M., "2-D Array Experiment on Board a Space Flyer Unit," *Space Solar Power Review*, Vol. 5, March 1985, pp. 345–356.

[15]Natori, M. C., Kuninaka, H., Higuchi, K., Kawai, Y., and Ikegami, S., "Two-Dimensionally Deployable High Voltage (2D/HV) Solar Cell Array Experiment in Space," AIAA Paper 95-1512, April 1995.

[16]Natori, M. C., Kuninaka, H., Higuchi, K., and Onodera, T., "In-Orbit Deployment and Post Flight Analysis of the 2D Array On-board SFU," 48th International Astronautical Congress, Paper IAF-97-I.1.01, Oct. 1997.

[17]Leifer, J., Black, J. T., Belvin, W. K., and Behun, W., "Evaluation of Shear Compliant Borders for Wrinkle Reduction in Thin Film Membrane Structures," AIAA Paper 2003-1984, April 2003.

[18]Gaspar, J. L., Solter, M. J., and Pappa, R. S., "Membrane Vibration Studies Using a Scanning Laser Vibrometer," NASA TM-2002-211427, Feb. 2002.

[19]Slade, K. N., and Belvin, W. K., "Solar Sail Loads, Dynamics, and Membrane Studies," AIAA Paper 2002-1265, April 2002.

[20]Pappa, R. S., Lassiter, J. O., and Ross, B. P., "Structural Dynamics Experimental Activities in Ultralightweight and Inflatable Space Structures," *Journal of Spacecraft and Rockets*, Vol. 40, No. 1, 2003, pp. 15–23.

[21]Slade, K. N., Belvin, W. K., Tetlow, T. K., and Behun, V., "Dynamic Characterization of a Subscale Solar Sail Using Non-Contacting Excitation and Sensing," AIAA Paper 2003-1744, April 2003.

[22]Holland, D. B., Virgin, L. N., and Belvin, W. K., "Investigation of Structural Dynamics in a 2-Meter Square Solar Sail Model Including Axial Load Effects," AIAA Paper 2003-1746, April 2003.

[23]Miller, R. K., and Hedgepeth, J. M., "An Algorithm for Finite Element Analysis of Partly Wrinkled Membranes," *AIAA Journal*, Vol. 20, No. 12, 1982, pp. 1761–1763.

[24]Jenkins, C. H., and Leonard, J. W., "Dynamic Wrinkling of Viscoelastic Membranes," *Journal of Applied Mechanics*, Vol. 60, Sept. 1993, pp. 575–582.

[25]Miyazaki, Y., and Nakamura, Y., "Dynamic Analysis of Deployable Cable–Membrane Structures with Slackening Members," 21st International Symposium on Space Technology and Science, Paper ISTS 98-b-13, May 1998.

[26]Liu, X., Jenkins, C. H., and Schur, W. W., "Large Deflection Analysis of Pneumatic Envelopes Using a Penalty Papameter Modified Material Model," *Finite Elements in Analysis and Design*, Vol. 37, No. 3, 2001, pp. 233–251.

[27]Adler, A. L., Mikulas, M. M., and Hedgepeth, J. M., "Static and Dynamic Analysis of Partially Wrinkled Membrane Structures," AIAA Paper 2000-1810, April 2000.

[28]Adler, A. L., and Mikulas, M. M., "Application of a Wrinkled Membrane Finite Element Approach to Advanced Membrane Structures," AIAA Paper 2001-4646, Aug. 2001.

[29]Johnston, J., "Finite Element Analysis of Wrinkled Membrane Structures for Sunshield Applications," AIAA Paper 2002-1456, April 2002.

[30]Kukathasan, S., and Pellegrino, S., "Nonlinear Vibration of Wrinkled Membranes," AIAA Paper 2003-1747, April 2003.

[31]Miyazaki, Y., and Uchiki, M., "Deployment Dynamics of Inflatable Tube," AIAA Paper 2002-1254, April 2002.

[32]Chopra, A. K., *Dynamics of Structures*, Prentice–Hall, Englewood Cliffs, NJ, 1995, Chap. 11.

[33]Natori, M., Miura, K., Ichida, K., and Kuwao, F., "Vibration Control of Membrane Space Structures Through the Change of Support Tension," 40th Congress of the International Astronautical Federation, Paper IAF-89-335, Oct. 1989.

[34]Solter, M. J., Horta, L. G., and Panetta, A. D., "A Study of a Prototype Actuator Concept for Membrane Boundary Control," AIAA Paper 2003-1736, April 2003.

G. Agnes
Associate Editor